

See discussions, stats, and author profiles for this publication at: <https://www.researchgate.net/publication/51080777>

Nobilamides A–H, Long-Acting Transient Receptor Potential Vanilloid-1 (TRPV1) Antagonists from Mollusk-Associated Bacteria

ARTICLE *in* JOURNAL OF MEDICINAL CHEMISTRY · JUNE 2011

Impact Factor: 5.45 · DOI: 10.1021/jm101621u · Source: PubMed

CITATIONS

16

READS

36

10 AUTHORS, INCLUDING:



Zhenjian Lin

University of Utah

37 PUBLICATIONS 578 CITATIONS

SEE PROFILE



Christopher A Reilly

University of Utah

60 PUBLICATIONS 1,184 CITATIONS

SEE PROFILE



Gisela Concepcion

University of the Philippines Diliman

88 PUBLICATIONS 1,311 CITATIONS

SEE PROFILE



Margo G Haygood

Oregon Health and Science University

69 PUBLICATIONS 3,181 CITATIONS

SEE PROFILE

Published in final edited form as:

J Med Chem. 2011 June 9; 54(11): 3746–3755. doi:10.1021/jm101621u.

Nobilamides A-H, Long-Acting Transient Receptor Potential Vanilloid-1 (TRPV1) Antagonists from Mollusk-Associated Bacteria

Zhenjian Lin[†], Christopher A. Reilly[§], Rowena Antemano[±], Ronald W. Hughen[‡], Lenny Marett[†], Gisela P. Concepcion[±], Margo G. Haygood[†], Baldomero M. Olivera^{||}, Alan Light[‡], and Eric W. Schmidt^{*,†,||}

[†] Department of Medicinal Chemistry, University of Utah, Salt Lake City, Utah 84112, USA

[§] Department of Pharmacology and Toxicology, University of Utah, Salt Lake City, Utah 84112, USA

[‡] Department of Anesthesiology, University of Utah, Salt Lake City, Utah 84112, USA

^{||} Department of Biology, University of Utah, Salt Lake City, Utah 84112, USA

[±] Marine Science Institute, University of the Philippines, Diliman, Quezon City 1101, Philippines

[†] Department of Environmental and Biomolecular Systems, OGI School of Science & Engineering, Oregon Health & Science University, Beaverton, Oregon 97006, USA

Abstract

New compounds nobilamides A-H and related known compounds A-3302-A and A-3302-B were isolated based upon their suppression of capsaicin-induced calcium uptake in a mouse dorsal root ganglion primary cell culture assay. Two of these compounds, nobilamide B and A-3302-A, were shown to be long-acting antagonists of mouse and human TRPV1 channels, abolishing activity for >1 h after removal of drug presumably via a covalent attachment. Other derivatives also inhibited the TRPV1 channel, albeit with low potency, affording a structure-activity profile to support the proposed mechanism of action. While the activities were modest, we propose a new mechanism of action and a new site of binding for these inhibitors that may spur development of related analogs for treatment of pain.

Keywords

TRPV1; D-amino acid; depsipeptide

INTRODUCTION

More than 30 Transient Receptor Potential (TRP) channels are known, including many which are important in sensing stimuli such as cold, heat, and pain. Among these, TRP

*To whom correspondence should be addressed. Mailing address: College of Pharmacy, Medicinal Chemistry, 307 Skaggs Hall, 30 S. 2000 E., Rm. 201, Salt Lake City, Utah 84112-5820. Phone: (801) 585-5234. Fax: (801) 585-9119., ewsl@utah.edu.

Supporting Information

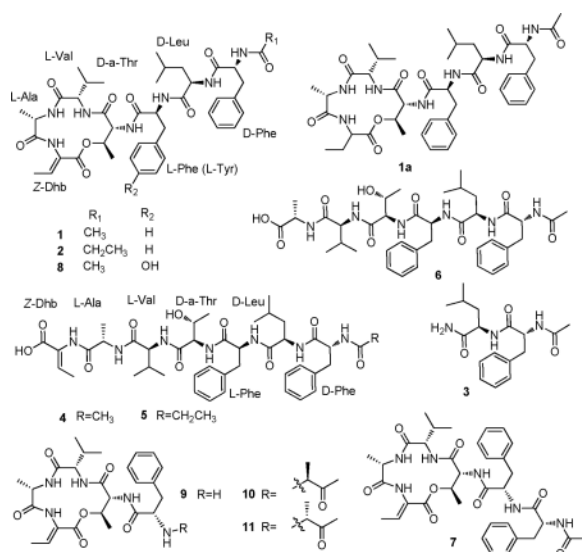
Materials and Methods for chemistry and isolation, Marfey's analysis, and NMR and MS data. This material is available free of charge via the Internet at <http://pubs.acs.org>.

^aAbbreviations: TRPV1 (VR1), Transient Receptor Potential Vanilloid-1; HEK-239, human embryonic kidney cell line; CGRP, calcitonin gene-related peptide; DRG, dorsal root ganglion; BEAS-2B, human bronchial epithelial cell line; HRESIMS, high-resolution electrospray ionization mass spectrometry.

Vanilloid-1 (TRPV1; VR1) is a nonselective cation channel that is a major mediator of pain and inflammation.¹ Stimuli such as heat, protons, and chemical ligands provoke action potentials, leading to the release of neurotransmitters and neuroactive peptides (e.g., substance P, neurokinin A, and CGRP) from peripheral and central nerve terminals.² Many lines of experimental evidence indicate that selective TRPV1 antagonism could play a useful role in the treatment of chronic pain and inflammatory hyperalgesia.^{3,4} Indeed, many such ligands have been reported and have entered clinical and preclinical trials.^{4,5} Endovanilloids and the endogenously supplied ligand, capsaicin, are potent TRPV1 activators that cause sensations of heat and pain in the short term, but lead to pain desensitization in the longer term.⁶ Vanilloids such as capsaicin bind at an intramembrane and intracellular site located between TM segments 3 and 4, involving Y511, S512, W549, and other residues.⁷ This site is distinct from the channel pore-loop segment but binding of ligands to this site is presumed to induce structural changes in the pore loop region such that ions can pass through the tetrameric receptor pore. Antagonists that compete with vanilloids are among the major drug leads so far identified. However, recently selective agonists that bind directly to the channel region have also been identified.⁸ Because of the varied physiological responses to individual agonists and antagonists, there is still a need for further agents for clinical and biological investigation.

TRPV1 is among the important channels found in dorsal root ganglion (DRG) neurons, which transfer afferent signals such as pain, heat, and touch.⁹ These neurons also contain many other types of channels and receptors, making them excellent models for broad-net drug discovery assays. We employ an assay using a primary culture of mouse DRG neurons containing many of the different cell types normally present in the DRG of live mice.¹⁰ Cells are exposed to a series of treatments including KCl and chemical extracts or pure compounds. By observing differences in the resulting Ca^{2+} flux, we have discovered compounds that act directly on channels and receptors important in transferring information about pain, heat, touch, and other properties. For example, using this assay, we recently reported the identification of potent and selective ligands for the serotonin 5-HT_{2B} receptor.¹¹

One of the advantages of the DRG assay is that cell types containing distinct receptor and channel populations can be pharmacologically distinguished. For instance, application of capsaicin differentiates nociceptors from other cell types. In the course of screening bacterial extracts for DRG activity, the organic extract of strain *Streptomyces* sp. CN48 produced a novel effect; in addition to strongly increasing Ca^{2+} in DRG neurons in response to KCl addition, the extract inactivated all response to capsaicin, even 2 min after removal of the extract. It was thus proposed that this extract might irreversibly inactivate TRPV1 through a possibly novel mechanism. Here, we report discovery and structure elucidation of eight new peptides, nobilamides A-H (**4–11**) and two related known compounds A-3302-A (**1**) and A-3302-B (**2**), that produce long-term (>1 h) inhibition of TRPV1. Their effects on endogenously expressed and recombinant wild-type and mutant human TRPV1 channels were assessed, showing that the compounds function by a mechanism that appears to involve covalent modification of TRPV1 through residues that constitute an intracellular helix spanning TM4 and 5 and the pore-loop segment. Although the compounds are not exceptionally potent, they provide lead structures for the development of a new class of TRPV1 antagonists.



RESULTS AND DISCUSSION

Bioassay-Guided Purification

Strains CN48 and CT3a were cultivated from dissected tissues of the mollusks *Chicoreus nobilis* and *Conus tribblei*, respectively, from Cebu, Philippines. Informed local and national consent and intellectual property agreements were obtained prior to performing this study. 16S gene sequence analyses showed that both strains belong to the genus *Streptomyces*. Sequences were deposited in GenBank, accession numbers, HQ696493 (CN48), HQ696492 (CT3a).

Crude extracts of CN48 and CT3a were strongly active in the DRG assay. The CN48 extract strongly activated DRG cells upon addition of KCl, while that from CT3a was strongly deactivating. Moreover, the CN48 extract blocked activation by capsaicin. Despite these differences, HPLC analysis showed that the two strains contained closely related families of metabolites, which were further purified by bioassay- and chemistry-guided fractionation. Following fermentation, cells were pelleted by centrifugation, and the resulting broths were subjected to HP20 resin adsorption chromatography. The moderately polar fractions were further purified by C₁₈ flash chromatography followed by C₁₈ HPLC to yield compounds **1**–**11**.

Structure Elucidation

By comparison of spectroscopic data and physicochemical properties with literature reports, two compounds **1** and **2** were identified as the previously reported metabolites, A-3302-B (also known as TL-119) and A-3302-A.¹² Another isolated compound **3**, *N*-acetyl-L-phenylalanyl-L-leucinamide, has been synthesized but is not previously known as a natural product;¹³ in this case **3** is instead composed of D-amino acids (see below).

The molecular formula of **4** was determined as C₄₂H₅₉N₇O₁₀ by high-resolution electrospray ionization mass spectrometry (HRESIMS) and ¹H and ¹³C NMR data (Tables 1 and 2), indicating that it was larger than **1** by H₂O. In addition, the NMR data of **4** were largely identical to those of the known compound **1**. In fact, the only major difference was that the threonine β-methine ¹H and ¹³C resonances of **4** were shifted 0.8 ppm and 5 ppm upfield in comparison to those of **1**. This difference led us to propose that **4** was a linear peptide lacking the lactone linkage found in **1**. To confirm this hypothesis, we performed a

complete analysis of 1D and 2D NMR data (supporting information), showing that **4** contained the same amino acid residues in the same order as **1**: α,β -dehydrobutyryne (Dhb), alanine (Ala), valine (Val), threonine (Thr), leucine (Leu), and two phenylalanines (Phe). Additionally, like **1**, **4** was acetylated at its N-terminus.

Compound **5** was assigned the molecular formula $C_{43}H_{61}N_7O_{10}$ on the basis of HRESIMS analysis and NMR experiments (Tables 1 and 2), making it larger than **2** by H_2O and larger than **4** by CH_2 . Detailed analysis of 1H - 1H COSY and HMBC NMR experiments indicated that **5** differed from **4** only by the absence of an acetyl group; instead, a propionyl group (δ_H 1.98, 2H; 0.82, 3H) was assigned to **5**. Analysis of 2D NMR data of **5** confirmed the presence of propionyl group and defined the amino acid sequence. Compound **5** is identical to the known compound **2**, except that it is linear instead of a cyclic depsipeptide. Although **4** and **5** are only trivial derivatives of the known compounds **1** and **2**, careful HPLC analysis indicates that they are indeed present in the fermentation media during the normal course of bacterial growth in the same ratios found after chemical isolation. Thus, they are naturally produced by these strains under these experimental conditions and are not extraction artifacts.

Compound **6** was found to possess the molecular formula $C_{38}H_{54}N_6O_9$ by analysis of HRESIMS and NMR data (Tables 1 and 2). The difference in the molecular formula of C_4H_5NO from **4** was attributed to the absence of the Dhb residue. The 1H NMR of **6** lacked the olefinic proton signal at about 6.5 ppm found in **4** and **5**. Analysis of NMR data confirmed the absence of the Dhb residue and allowed assignment of the amino acid sequence for **6**.

Compound **7** was assigned the molecular formula $C_{36}H_{46}N_6O_8$ on the basis of HRESIMS analysis and NMR experiments (Tables 1 and 2). The NMR data of **7** were closely related to those of **1**. The chemical shifts of the Thr β -methine group were observed at δ_H 4.72 and δ_C 73.9, which indicated that **7** was a cyclic peptide with a lactone linkage between the C-terminal amino acid and the hydroxyl group of the Thr residue. Further analysis of the NMR data of **7** showed that, in comparison to **1**, Leu was absent. A NOESY correlation between protons at 4.48 ppm and 8.42 ppm established the connection between the two Phe residues in place of Leu.

The molecular formula of **8** was determined as $C_{42}H_{57}N_7O_{10}$ by high resolution ESIMS coupled with 1H and ^{13}C NMR data (Tables 1 and 2). The difference in the molecular formula of an oxygen atom from **1** was attributed to the presence of a tyrosine (Tyr) residue in place of Phe. The 1H NMR spectrum of **8** showed a pair of aromatic doublets δ_H 7.00, 6.62, which were assigned to Tyr. The ^{13}C NMR spectrum (Table 2) of **8** also indicated an oxygenated phenyl carbon at δ_C 156.5. HMBC and NOESY NMR data were consistent with the proposed structure of **8**.

Compound **9** was assigned the molecular formula $C_{25}H_{35}N_5O_6$ on the basis of HRESIMS analysis and NMR experiments (Tables 1 and 2). The difference in the molecular weight in comparison to **1** was attributed to the absence of two amino acid residues (Leu and Phe) and an acetyl group from the N-terminus of the peptide. Compatibly, the NMR data (Tables 1 and 2) of **9** showed the absence of those signals for the two amino acid residues and acetyl group. Analysis of HMBC and NOESY NMR data confirmed the amino acid sequence of **9**.

Compounds **10** and **11** were isolated with very similar HPLC retention times. The molecular formula for both was determined as $C_{29}H_{41}N_5O_7$ by high resolution ESIMS coupled with NMR data (Tables 1 and 2). The 1H and ^{13}C NMR data of **10** and **11** showed similar NMR signals (Tables 1 and 2), suggesting they might be isomers of each other. In comparison the 1H and ^{13}C NMR data (Tables 1 and 2) to that of **9**, two more methyl groups (δ_H 2.14,

H-3, δ_C 27.8, C-3 and δ_H 1.17, H-4, δ_C 19.3, C-4) and a methine group (δ_H 3.42, H-1, δ_C 64.7, C-1) were present. The distinctive methyl singlet at δ_H 2.14 corresponded to an α -keto methyl group, but no ketone carbon was observed in the ^{13}C NMR spectrum (Table 2) of **10**. In the HMBC spectrum of **10**, two strong correlations were observed from both H-3 and H-4 to a ketone carbon at 215.3 ppm, indicating a $-\text{CH}(\text{CH}_3)\text{COCH}_3$ fragment. Further HMBC correlations from H-1 to the α -C (δ_C 64.9) of Phe, and from the α -H (δ_H 3.30) of Phe to C-1 indicated the connection of these two partial structures. The same features were found in the NMR data of **11**. Therefore, compound **11** had the same planar structure as **10**.

Absolute configuration was assigned using Marfey's method.¹⁴ Compounds **4–11** were hydrolyzed, and the resulting amino acids were converted to *N* α -(2,4-dinitro-5-fluorophenyl)-L-alaninamide derivatives, which were characterized by HPLC in comparison with authentic standards. Compounds **4–6** contain L-Ala, L-Val, D-*allo*-Thr, D-Leu, and L- and D-Phe. In comparison to **4–6**: **7** is identical but lacks D-Leu; **8** contained L-Tyr in place of L-Phe; and **9–11** lacked D-Phe and D-Leu. **3** consisted solely of D-Leu-D-Phe. When both L- and D-Phe were present, the order could not be ascertained from these experiments. However, **1** was previously synthesized¹² and was found in both the cultures of CT3a and CN48. We propose that the absolute configurations of **1–11** are identical. This hypothesis was further supported by comparison with the configurations of **7–11**, which were completely defined experimentally and in which only one Phe residue was present. For **10** and **11**, the configurations of the terminal ketone moieties are speculative.

Compounds **1–11** are closely related to each other, belonging to a family that was previously only known from *Bacillus subtilis*.^{15,16} There were a few noteworthy modifications. Compound **6** is related to **4** just by the loss of Abu; this may be due to enzymatic hydrolysis post-synthesis or to imperfect product synthesis by biosynthetic enzymes. In comparison to **1**, **7** is missing a Leu that is within the peptide sequence itself. If the compounds are indeed produced nonribosomally, this may be due to module skipping.¹⁷ Compounds **10**, and **11**, are related to the rest by loss of the two N-terminal amino acids, which are instead replaced by an unprecedented ketone derivative. A similar type of modification was recently described for an unrelated natural compound.¹⁸

Capsaicin Antagonism in the Mouse DRG Assay

The fluorometric calcium flux DRG assay allows for the simultaneous study of 100–150 neurons with single application of compounds. Multiple neuronal cell types are present in each well, including a substantial fraction of nociceptors (~30–50%); each cell type has different combinations of receptors and channels and exhibits a different pharmacological profile.¹⁰ In the standard discovery assay, responses elicited by chemicals are normalized by pulsing with 25 mM KCl, which leads to depolarization, followed by washout, bringing cells back to baseline. Subsequently, samples of extracts or pure compounds are added to observe any direct depolarizing effects, then samples are added in tandem with 25 mM KCl to observe any increase or decrease of depolarization. After a washout period, capsaicin (a TRPV1 agonist) is added to differentiate nociceptors from other cell types. Finally, a pulse of 100 mM KCl is added to determine whether cells are still responding normally and to obtain a value for maximum depolarization. By following changes in intracellular Ca^{2+} over these steps, fine information about the activity of extracts is revealed, enabling discovery of new agents.

Using the above procedure, application of a major fraction of *Streptomyces* sp. CN48 extract led to a complete loss of response to capsaicin, but subsequent addition of 100 mM KCl still strongly depolarized all neurons in assay wells, indicating that they otherwise were alive and functioning normally. In addition, the extract was mildly stimulating to cells when co-applied with 25 mM KCl. In a pure compound test, 5 min after application of purified **4** at a

final concentration of 125 μ M, the DRG cells were depolarized by 25 mM KCl, and after that a complete loss of response to capsaicin was observed. Based upon these results, we proposed that the nobilamides in the CN48 extract were responsible both for increased depolarization of DRG cells and for inhibition of response to capsaicin.

Nobilamides Induce Long-Term Changes in TRPV1

Two likely mechanisms could explain the DRG results. In the first, nobilamides could impact regulatory proteins that reduce capsaicin receptor activity. In the second, due to the long delay prior to addition of capsaicin, it was possible that nobilamides irreversibly inactivated capsaicin receptors. We therefore tested individual compounds in assays using human bronchial epithelial BEAS-2B cells, which stably overexpress human TRPV1, primarily intracellularly.^{19–22} Direct competition experiments indicated that compounds **2** and **5** antagonize the action of capsaicin on TRPV1 (supporting information), with an apparent preference for cell-surface localized channels. Onset of action was slow, and pre-incubation led to substantially greater activity versus co-application. However, with this cell line we could not determine whether this delayed effect might be due to a slow on-rate (such as found in some irreversible inhibitors) or whether cell penetration was a limiting factor for these large peptides. Therefore, we used HEK-293 cells transfected with human TRPV1. This cell line does not normally express capsaicin-sensitive channels, and upon transfection TRPV1 is expressed largely on the cell surface, making it possible to measure inhibition in the absence of potential confounding effects. In this cell line, the potency of **5** was greatly increased with pre-incubation of the compounds prior to capsaicin application, in comparison to co-application with capsaicin (Figure 1). This observation was consistent with an irreversible binding model. In a series of further experiments, the inhibitory activity of **5** was found to be stable through four washes taking place over a 60-min period (Figure 2). However, a slight rebound of activity was noticed after one hour in these human cells, indicating either a slow reversibility or replacement of inhibited TRPV1 by newly synthesized protein.

To further examine this effect, we investigated the long-term antagonism of mouse DRG neurons, in an assay adapted to allow lengthy survival and monitoring of capsaicin responses in individual neurons (100–150 per well). In the first experiment, mouse DRG neurons were incubated with compound **4**, then allowed to recover over a three-hour period. Although the capsaicin response was initially abolished, recovery was observed after three hours. To determine whether recovery was due to new protein synthesis, TRPV1 recycling, or slow reversibility of binding, cells were also treated with actinomycin D, cycloheximide, and brefeldin A under several different conditions to inhibit transcription, translation, and trafficking of TRPV1 to the cell surface and subjected to the same 3-hour recovery experiment. Individual neurons were followed for the entire duration of the experiment so that recovery of single cells would be observable. Response to capsaicin was restored after three hours, indicating that channel synthesis or turnover was likely not involved in recovery, and that instead tightly or covalently bound **4** was slowly released over this time course. Thus, it can be concluded that nobilamides are long-acting antagonists of TRPV1, probably through a covalent modification of the receptor. Because *agonists* that act for >15 min on TRPV1 have previously been termed “essentially irreversible”,⁸ we propose that nobilamides represent a class of essentially irreversible antagonists.

Nobilamides Block TRPV1 Channel at a Novel Site

Because the inhibitory nobilamides contain the modest electrophile, dehydrobutyrine, it seemed possible that the compounds might covalently modify nucleophiles in TRPV1, leading to inhibition. Indeed, we reduced the dehydrobutyrine residue of **1** with H₂, and the resulting **1a** was completely inactive. Candidate nucleophiles included cysteine (Cys)

residues in the pore loop region, which were previously shown to be important redox-sensitive residues. TRPV1 is very active in reducing conditions, and its activity greatly decreases through Cys disulfide formation in the channel under more oxidizing conditions.²³ In addition, other TRP channels have been found which are agonized or antagonized by relatively non-specific electrophiles.²⁴

To test the site of binding and the possibility of covalent modification, HEK-239 cells overexpressing mutant human TRPV1 variants were treated with compounds **2** and **5** (Figure 3). Six mutants were used. Of these, three were inhibited by **2** and **5** in a manner similar to wild type, while three exhibited significantly reduced inhibition by **2** or **5**. Two Cys mutants (C578A and C621A) and the F660A mutant, adjacent to the ion conducting pore of TRPV1,²⁵ led to a complete loss of TRPV1 antagonism. These results suggest that **2** and **5** bind directly to the pore-loop segment of the channel, where they act as channel blockers by either modifying local protein dynamics required for activation and/or ion flux or as a “molecular blockade” via the formation of covalent adducts that possibly bridge TRPV1 subunits to prevent ion flux from occurring. It is curious that removing either Cys residue abolishes the antagonist response, which defies simple models of single alkylation. Moreover, incubation of nobilamides with glutathione did not impact activity, indicating that the dehydrobutyrine residue is at most a modestly active electrophile that requires appropriate steric directing by adjacent residues such as F660 on TRPV1. We propose that nobilamides covalently inactivate TRPV1 based upon: 1) the lack of activity when the electrophile Dhb was reduced or absent; 2) the requirement for Cys residues in the binding site; 3) the slow onset time for activity; and 4) the extremely long duration of binding. Whether binding is covalent or not, and indeed whether or not it involves 1:1 stoichiometry, the compounds essentially irreversibly inhibit TRPV1 at a novel site of action.

Covalent Cys modification is important for rodent TRPV1 *agonists* such as allicin and nitric oxide, which act primarily on C157 of the rat proteins.^{26,27} These activating effects are relatively short lived and readily reversible in comparison to the inactivating effect of nobilamides, which are long lasting and act in a wholly different region of the protein. By further contrast, a pore-loop Cys residue (C621) impacting nobilamide activity in human TRPV1 potentiates the response of the rat channel to heat.²⁸ F660 is required for acid sensitivity, and mutations of this residue completely abolish this response while maintaining capsaicin sensitivity.²⁹ Very recently, data were obtained indicating that F660 is probably primarily involved in gating the response to protons.³⁰ It is interesting that nobilamides apparently directly act on or are affected by amino acids that potentiate the response to important additional TRPV1 activators. Based upon these results, we propose that the nobilamides block the pore such that they antagonize activation by many different activators including capsaicin, heat, and protons. Direct channel blocking antagonists, such as tetrabutylammonium,³¹ have been previously described, but these in general exhibit lower potency than nobilamides, lack selectivity, and are readily reversible.

Structure-Activity Relationships

Persistent human and mouse TRPV1 antagonism was observed at relatively high nobilamide concentrations (above 200 μ M, in comparison to an activating capsaicin concentration of 2–25 μ M in these cell lines). However, this activity was highly selective, and slight differences in structure led to complete abrogation of activity. Of these compounds, only **1**, **2**, **4**, and **5** exhibited inhibitory activity. In fact, very slight modifications led to large activity differences. Compounds **1** and **4** exhibited relatively low activity, with IC₅₀ values of 1320 and 1665 μ M, respectively. However, **2** and **5** were much more potent, with IC₅₀ values of 227 and 275 μ M, respectively. The only difference between **2/5** and **1/4** is that the former are longer by a single methylene group. By contrast, the existence of a constraining ester does not appear to be highly important in conferring activity. Neither **6** nor **1a** exhibited

detectable activity, indicating the importance of the intact dehydrobutyrine residue. Additionally, **7**–**11**, which differed only by length or residue in the side chain, were totally inactive. Strikingly, the only difference between active **1** and inactive **8** was the presence of OH (Tyr) in place of H (Phe) in the side chain. **7** was lacking only a single Leu residue in the side chain. These results reinforce the selective nature of inactivation and indicate that inhibition is not due to a simple and nonspecific covalent modification.

In conclusion, these results demonstrate that nobilamides antagonize TRPV1 and highlight the possibility of engineering more potent analogs that block the TRPV1 channel in this novel manner. Very slight differences in amino acids or in the N-terminus of the peptides exert large effects on activity, so that synthesis of analogs is promising. Moreover, within the natural derivatives the amino acid sequence is relatively fixed; there is much room for modification by making substitutions. The presence of D-amino acids in key positions is also a great benefit to design of more potent analogs, since D-peptides are known to be more stable than their L-counterparts in human use.³² Finally, irreversibility itself may prove to be an advantage.

Experimental Section

General—UV spectra were obtained using a Perkin-Elmer Lambda2 UV/vis spectrometer. IR spectra were recorded on a JASCO FT/IR-420 spectrometer. NMR data were collected using either a Varian INOVA 500 (¹H 500 MHz, ¹³C 125MHz) NMR spectrometer with a 3 mm Nalorac MDBG probe or a Varian INOVA 600 (¹H 600 MHz, ¹³C 150 MHz) NMR spectrometer equipped with a 5 mm ¹H[¹³C, ¹⁵N] triple resonance cold probe with a z-axis gradient and utilized residual solvent signals for referencing. High-resolution mass spectra (HRMS) were obtained using a Bruker (Billerica, MA) APEXII FTICR mass spectrometer equipped with an actively shielded 9.4 T superconducting magnet (MagneX Scientific Ltd., UK), an external Bruker APOLLO ESI source, and a Synrad 50W CO₂ CW laser. All compounds were assessed to be >99% pure by HPLC with DAD and MS detectors.

Fermentation and Extraction—Strains CN48 and CT3a were each individually grown at 30 °C with shaking at 200 rpm in a 10 L fermentor containing 10 L of ISP2 medium (0.2% yeast extract, 1% malt extract, 0.2% glucose, 2% NaCl). After 8 days, the broth was centrifuged and the supernatant was extracted with HP-20 resin for 4 hours. The resin was filtered through cheesecloth, washed with water to remove salts, and eluted with MeOH to yield the crude extract.

Purification—The crude extract (650 mg) of CN48 was separated into 5 fractions (Fr1–Fr5) on a C₁₈ column using gradient elution of MeOH in H₂O (50%, 60%, 70%, 80%, 100%). Fr4 eluting in 80% MeOH was further purified by C₁₈ HPLC using 85% MeOH in H₂O to obtain **4** (100.0 mg) and **6** (4.0 mg), and two further fractions Fr4-3 and Fr4-4. Fr4-3 was further purified by C₁₈ HPLC using 37% CH₃CN in H₂O with 0.1% TFA to obtain **5** (2.0 mg), **7** (1.0 mg), and **8** (1.2 mg). Fr4-4 was further purified by C₁₈ HPLC using 45% CH₃CN in H₂O with 0.1% TFA to obtain **1** (150.0 mg). Fraction Fr5 was further purified by C₁₈ HPLC using 55% CH₃CN in H₂O with 0.1% TFA to obtain **2** (1.0 mg).

The crude extract (350 mg) of CT3a was separated into 5 fractions (Fr1–Fr5) on a C₁₈ column using gradient elution of MeOH in H₂O (20%, 40%, 60%, 70%, 80%). Fr4 eluting in 70% MeOH was further purified by C₁₈ HPLC using 39% CH₃CN in H₂O to obtain **9** (1.5 mg), **10** (2.0 mg) and **11** (3.0 mg). Compound **3** was obtained from fraction Fr2 by C₁₈ HPLC using 25% CH₃CN in H₂O. In addition, compounds **4** (1.0 mg) and **1** (0.4 mg) were also isolated from fraction Fr5 of CT3a.

Compound 1a—Compound **1** (1.0 mg) in methanol (2.0 mL) was treated with a balloon of H₂ gas and 10% palladium on carbon (3 mg) overnight. The reaction mixture was filtered through silica gel, evaporated to dryness, and purified by HPLC (80% methanol in H₂O with 0.1% TFA) to give **1a** (0.4 mg; 40% isolated yield): white solid; ¹H NMR (DMSO, 500 MHz), L-Phe: δ 4.63 (1H, m, α-H), 3.27 (2H, m, β-H), 6.96–7.27 (5H, m, Ph-H); D-Phe: δ 4.65 (1H, m, α-H), 2.68 (1H, dd, *J* = 14.1, 5.0 Hz, β-H₁), 6.96–7.27 (5H, m, Ph-H); 4.67 (1H, dd, *J* = 9.5, 5.2 Hz, α-H, Phe), 4.45 (1H, t, *J* = 7.6 Hz, α-H, Leu), 2.92 (1H, dd, *J* = 14.1, 10.0 Hz, β-H₂), 6.96–7.27 (5H, m, Ph-H); L-Val: δ 3.94 (1H, m, α-H), 2.06 (1H, m, β-H), 0.86 (3H, d, *J* = 6.5 Hz, γ-Me), 0.79 (3H, d, *J* = 6.5 Hz, γ-Me); But: δ 4.23 (1H, m, α-H), 1.57 (2H, m, β-H), 0.72 (3H, t, *J* = 7.5 Hz, γ-Me); L-Ala: δ 3.76 (1H, m, α-H), 1.04 (3H, d, *J* = 6.8 Hz, β-Me); D-Leu: δ 3.92 (1H, m, α-H), 1.22 (2H, m, β-H), 1.20 (1H, m, γ-H), 0.81 (6 H, d, *J* = 6.5 Hz, d-Me); D-a-Thr: δ 4.20 (1H, m, α-H), 4.21 (1H, m, β-H), 1.30 (3H, d, *J* = 6.5 Hz, γ-Me); δ 1.91 (3H, s, acetyl); ESIMS *m/z* 806 [M+H]⁺, 828 [M+Na]⁺.

N-Acetyl-L-phenylalanyl-L-leucinamide (3)—colorless solid; ¹H NMR (CDCl₃, 500 MHz) δ 7.18–7.28 (5H, m, Ph-H, Phe), 4.67 (1H, dd, *J* = 9.5, 5.2 Hz, α-H, Phe), 4.45 (1H, t, *J* = 7.6 Hz, α-H, Leu), 3.17 (1H, dd, *J* = 14.1, 5.0 Hz, β-H₁, Phe), 2.85 (1H, dd, *J* = 14.1, 10.0 Hz, β-H₂, Phe), 1.88 (3H, s, acetyl group), 1.71 (1H, m, γ-H, Leu), 1.64 (2H, m, β-H, Leu), 0.96 (3H, d, *J* = 6.5 Hz, Me, Leu), 0.92 (3H, d, *J* = 6.5 Hz, Me, Leu); ¹³C NMR (CDCl₃, 125 MHz) δ 174.5 (C, COOH, Leu), 172.6 (C, C=O, Phe), 171.9 (C, C=O, acetyl group), 137.3 (C, Ph-C, Phe), 129.1 (CH, Ph-CH, Phe), 128.2 (CH, Ph-CH, Phe), 126.5 (CH, Ph-CH, Phe), 54.7 (CH, α-CH, Phe), 50.9 (CH, α-CH, Leu), 40.5 (CH₂, β-CH₂, Leu), 37.7 (CH₂, β-CH₂, Phe), 24.8 (CH, γ-CH, Leu), 22.2 (CH₃, acetyl group), 21.1 (CH₃, Leu), 20.7 (CH₃, Leu). ESIMS *m/z* 321 [M+H]⁺.

Nobilamide A (4)—white solid; [α]_D²⁰ −20 (c 0.1, DMSO); UV (MeOH) λ_{max} (logε) 210 (3.9), 243 (1.2) nm; IR (film) ν_{max}: 3272, 2978, 1808, 1712, 1696, 1648, 1568, 1553, 1537, 1112, 984 cm^{−1}; ¹H and ¹³C NMR, see Tables 1 and 2; HRESIMS *m/z* 844.4232 [M+Na]⁺ (calcd for C₄₂H₅₈N₇O₁₀Na, 844.4216, δ = −1.9 ppm).

Nobilamide B (5)—white solid; [α]_D²⁰ +3 (c 0.01, DMSO); UV (MeOH) λ_{max} (logε) 210 (4.0), 243 nm (1.3); IR (film) ν_{max}: 3276, 2923, 1753, 1692, 1630, 1568, 1553, 1538, 1107, 985 cm^{−1}; ¹H and ¹³C NMR, see Tables 1 and 2; HRESIMS *m/z* 858.4418 [M+Na]⁺ (calcd for C₄₃H₆₀N₇O₁₀Na, 858.4372, δ = −5.4 ppm).

Nobilamide C (6)—white solid; [α]_D²⁰ −15 (c 0.1, DMSO); UV (MeOH) λ_{max} (logε) 210 (3.9), 243 (1.1) nm; IR (film) ν_{max}: 3142, 2936, 1652, 1648, 1520, 1510, 1272, 1016 cm^{−1}; ¹H and ¹³C NMR, see Tables 1 and 2; HRESIMS *m/z* 761.3889 [M+Na]⁺ (calcd for C₃₈H₅₃N₆O₉Na, 761.3844, δ = 5.9 ppm).

Nobilamide D (7)—white solid; [α]_D²⁰ −24 (c 0.1, DMSO); UV (MeOH) λ_{max} (logε) 210 (3.8), 255 (1.5) nm; IR (film) ν_{max}: 3281, 2930, 1750, 1703, 1641, 1563, 1537, 1521 1265, 984 cm^{−1}; ¹H and ¹³C NMR see Tables 1 and 2; HRESIMS *m/z* 713.3334 [M+Na]⁺ (calcd for C₃₆H₄₅N₆O₈Na, 713.3270, δ = −9.0 ppm).

Nobilamide E (8)—white solid; [α]_D²⁰ −40 (c 0.01, DMSO); UV (MeOH) λ_{max} (logε) 210 (3.9), 256 (1.1), 276 (0.8) nm; IR (film) ν_{max}: 3296, 3062, 2968, 1664, 1648, 1563, 1547, 1531, 1249, 1016 cm^{−1}; ¹H and ¹³C NMR, see Tables 1 and 2; HRESIMS *m/z* 842.4095 [M+Na]⁺ (calcd for C₄₂H₅₆N₇O₁₀Na, 842.4059, δ = 4.3 ppm).

Nobilamide F (9)—white solid; [α]_D²⁰ −5 (c 0.1, DMSO); UV (MeOH) λ_{max} (logε) 210 (3.8), 255 (1.4) nm; IR (film) ν_{max}: 3124, 1703, 1672, 1688, 1452, 989 cm^{−1}; ¹H and ¹³C

NMR, see Tables 1 and 2; HRESIMS m/z 502.2666 $[M+H]^+$ (calcd for $C_{25}H_{36}N_5O_6$, 502.2660, $\delta = 1.2$ ppm).

Nobilamide G (10)—colorless solid; $[\alpha]_D^{20} -24$ (c 0.1, DMSO); UV (MeOH) λ_{max} ($\log \epsilon$) 210 (4.0), 255 (1.3) nm; IR (film) ν_{max} : 3278, 2926, 1754 1704, 1655, 1508, 1458, 983 cm^{-1} ; 1H and ^{13}C NMR, see Tables 1 and 2; HRESIMS m/z 572.3081 $[M+H]^+$ (calcd for $C_{29}H_{42}N_5O_7$, 572.3079, $\delta = 0.4$ ppm).

Nobilamide H (11)—colorless solid; $[\alpha]_D^{20} -27$ (c 0.1, DMSO); UV (MeOH) λ_{max} ($\log \epsilon$) 210 (4.0), 255 (1.4) nm; IR (film) ν_{max} : 3290, 2920, 1696, 1664, 1552, 1520, 1256, 1032 cm^{-1} ; 1H and ^{13}C NMR, see Tables 1 and 2; HRESIMS m/z 572.3079 $[M+H]^+$ (calcd for $C_{29}H_{41}N_5O_7$, 572.3079, $\delta = 0$ ppm).

DRG Assay—DRG cells from cervical and lumbar regions were obtained from C57B1 mice and used in an assay with bacterial culture extracts and pure compounds as previously described.¹⁰ Briefly, DRG cells were suspended in medium with additives and loaded with Fura-2 AM (Molecular Probes), a fluorescent dye used to measure intracellular calcium levels. Experiments were performed at room temperature (20 to 25°C) in a 24-well plate format using fluorescence microscopy. Individual cells were treated as single samples, so that the individual responses of diverse neuron subtypes from the DRG could be examined. After baseline measurements, the cells were treated with 25 mM KCl solution and then washed. After return to baseline, bacterial extracts, fractions, or pure compounds were applied. This solution was then later replaced with 25 mM KCl solution 5 min later. To differentiate pain-sensing and TRPV1-expressing neurons from other neuronal types, capsaicin was applied after return to baseline of the extracts. Finally, additional pulses of 25 mM KCl or 100 mM KCl were applied to determine whether cells were still viable with normal action potentials.

In long-term TRPV1 antagonism test, the cells were treated with capsaicin solution (100 or 200 nM) and then washed. After fluorescence returned to baseline, test compounds (125 μM) were applied and incubated for 5 min. The solution was decanted, and capsaicin solution (100 or 200 nM) was added, followed by a wash. After 3 hours, another capsaicin solution was applied. Finally, an additional pulse of KCl (100 mM) was applied to determine whether cells were still viable with normal action potentials. To test for protein synthesis and trafficking, cycloheximide (10 $\mu g/ml$), actinomycin D (6.3 $\mu g/ml$) and brefeldin A (5.6 $\mu g/ml$) were added either before or after compound application.

TRPV1 Assays—Cell-line based assays were performed using a BMG Labtech NOVOStar fluorescence plate reader equipped with a plate-to-plate reagent delivery system. Human immortalized bronchial epithelial (BEAS-2B) cells that stably overexpress human TRPV1 have been previously described.^{19–22} These cells express TRPV1 primarily intracellularly on the endoplasmic reticulum and exhibit an EC_{50} for capsaicin-induced calcium flux of 1–2 μM . Transiently transfected human embryonic kidney (HEK-293) cells were used for experiments involving overexpressed TRPV1 and mutants thereof. In these cells, TRPV1 is expressed primarily on the cell membrane.

BEAS-2B cells were grown to confluence in fibronectin/collagen/albumin coated 96-well plates in LHC-9 growth media, as previously described.^{19–22} Cells were prepared for the calcium flux assay by replacing the growth media with a 1:1 solution of LHC-9 and Fluo 4-Direct (Invitrogen) reagent containing Fluo 4-AM, pluronic F-127, probenecid, and a proprietary quencher dye. Cells were incubated at room temperature (~22°C) for 1h in the dark and subsequently washed by replacing the loading solution with LHC-9 containing 1 mM water-soluble probenecid (Invitrogen) and 750 μM Trypan Red (ATT Bioquest). For

pre-incubation experiments, test compounds were then added to the wash solutions in varying concentrations (described in figure legends). After 30 min incubation of cells at room temperature, assays were initiated by addition of capsaicin to a final concentration of 2.5 μM at 37°C (or 25 μM for HEK-293 cells). If test compounds were not pre-incubated, they were added concurrently with capsaicin. Changes in intracellular fluorescence (resulting from changes in cytosolic Ca^{2+}) were monitored for 1 min. Data were quantified in two ways. Rates were ($\Delta\text{F}/\text{sec}$) determined in comparison to the initial linear response observed in a control consisting of capsaicin only-treated cells. The magnitude of the response ($\Delta\text{F}_{\text{max}}$) observed for the entire 1 min time period was also calculated in comparison to control.

Human TRPV1 was cloned into the pcDNA3.1D V5/His vector (Invitrogen) and modified using the QuickChange site-directed mutagenesis kit (Stratagene). Mutations were confirmed by DNA sequencing. Plasmids (200 ng/well) were transfected into HEK-293 cells grown to confluence in 1% gelatin-coated 96-well plates using Lipofectamine 2000 (2:1 lipid:DNA ratio) prepared in OptiMEM media. Cells were cultured in the presence of the reagent for 4 h and cultured for 48 h in DMEM:F12 +5% FBS. After this time cells were processed and assayed for calcium flux as described above, except that the fluorophore loading steps were performed at 37°C.

Supplementary Material

Refer to Web version on PubMed Central for supplementary material.

Acknowledgments

This work was funded by ICBG grant U01TW008163 from Fogarty (NIH) (E.W.S.), NIH grant ES01734 (C.A.R.), and a seed grant from the Department of Anesthesiology, University of Utah (C.A.R.). We thank the government of the Philippines and the community of Mactan Island for permission to conduct this study.

References

1. Wu LJ, Sweet TB, Clapham DE. International Union of Basic and Clinical Pharmacology. LXXXVI. Current progress in the mammalian TRP ion channel family. *Pharmacol Rev.* 2010; 62:381–404. [PubMed: 20716668]
2. (a) Gazzieri D, Trevisani M, Springer J, Harrison S, Cottrell GS, Andre E, Nicoletti P, Massi D, Zecchi S, Nosi D. Substance P released by TRPV1-expressing neurons produces reactive oxygen species that mediate ethanol-induced gastric injury. *Free Radical Bio Med.* 2007; 43:1670.(b) Caterina MJ, Schumacher MA, Tominaga M, Rosen TA, Levine JD, Julius D. The capsaicin receptor: a heat-activated ion channel in the pain pathway. *Nature.* 1997; 389:816–824. [PubMed: 9349813]
3. Szallasi A, Appendino G. Vanilloid receptor TRPV1 antagonists as the next generation of painkillers. *J Med Chem.* 2004; 47:2717–2723. [PubMed: 15139748]
4. Malmberg, AB.; Bley, KR., editors. *Progress in Inflammation Research.* Birkhäuser-Verlag; Boston: 2005. *Turning up the Heat on Pain: TRPV1 Receptors in Pain and Inflammation.*
5. Gunthorpe MJ, Chizh BA. Clinical development of TRPV1 antagonists: targeting a pivotal point in the pain pathway. *Drug Discov Today.* 2009; 14:56–67. [PubMed: 19063991]
6. Jara-Oseguera A, Simon SA, Rosenbaum T. TRPV1: on the road to pain relief. *Curr Mol Pharmacol.* 2008; 1:255–269. [PubMed: 20021438]
7. Thomas K, Ethirajan M, Shahrokh K, Lee J, Cheatham T III, Sun H, Yost G, Reilly C. Structure-activity relationship of capsaicin analogs and transient receptor potential vanilloid 1-mediated human lung epithelial cell toxicity. *J Pharmacol Exp Ther.* 2011; 337:400–410. [PubMed: 21343315]

8. Bohlen CJ, Priel A, Zhou S, King D, Siemens J, Julius D. A bivalent tarantula toxin activates the capsaicin receptor, TRPV1, by targeting the outer pore domain. *Cell*. 2010; 141:834–845. [PubMed: 20510930]
9. Gallego-Sandin S, Rodriguez-Garcia A, Alonso MT, Garcia-Sancho J. The endoplasmic reticulum of dorsal root ganglion neurons contains functional TRPV1 channels. *J Biol Chem*. 2009; 284:32591–32601. [PubMed: 19778904]
10. Peraud O, Biggs JS, Huguen RW, Light AR, Concepcion GP, Olivera BM, Schmidt EW. Microhabitats within venomous cone snails contain diverse actinobacteria. *Appl Environ Microbiol*. 2009; 75:6820–6826. [PubMed: 19749071]
11. Lin Z, Antemano RR, Huguen RW, Tianero MDB, Peraud O, Haygood MG, Concepcion GP, Olivera BM, Light A, Schmidt EW. Pulicatin A-E, neuroactive thiazoline metabolites from cone snail-associated bacteria. *J Nat Prod*. 2010; 73:1922–1926. [PubMed: 21028889]
12. Kitajima Y, Waki M, Shoji J, Ueno T, Izumiya N. Revised structure of the peptide lactone antibiotic, TL-119 and/or A-3302-B. *FEBS Lett*. 1990; 270(1–2):139–142. [PubMed: 2226776]
13. Gorlero M, Wieczorek R, Adamala K, Giorgi A, Schinina ME, Stano P, Luisi PL. Ser-His catalyzes the formation of peptides and PNAs. *FEBS Lett*. 2009; 583:153–156. [PubMed: 19071124]
14. Marfey P. Determination of D-amino acids. II. Use of a bifunctional reagent, 1,5-difluoro-2,4-dinitrobenzene. *Carlsberg Res Commun*. 1984; 49:591–596.
15. Shoji J, Hino H, Wakisaka Y, Koizumi K, Mayama M. Isolation of a new peptide antibiotic TL-119. Antibiotics from the genus *Bacillus*. *J Antibiot*. 1975; 28:126–128. [PubMed: 1112764]
16. Ogawa Y, Mori H, Ichihashi M, Ueno T, Nakashima T, Fukami H, Kakajima R, Ida H. Structure elucidation of the antibiotics A-3302-A and -B produced by a new strain of *Bacillus subtilis*. *Peptide Chem*. 1977:123–126.
17. Wenzel SC, Meiser P, Binz TM, Mahmud T, Mueller R. Nonribosomal peptide biosynthesis: point mutations and module skipping lead to chemical diversity. *Angew Chem*. 2006; 45:2296–2301. [PubMed: 16506259]
18. Enomoto M, Kuwahara S. Total synthesis of bacilosarcins A and B. *Angew Chem*. 2009; 48:1144–1148. [PubMed: 19117003]
19. Thomas KC, Sllabnis AS, Johansen ME, Lanza DL, Moos PJ, Yost GS, Reilly CA. Transient receptor potential vanilloid 1 agonists cause endoplasmic reticulum stress and cell death in human lung cells. *J Pharmacol Exp Ther*. 2007; 321:830–838. [PubMed: 17332266]
20. Reilly CA, Johansen ME, Lanza DL, Lee J, Lim Ju-Ok, Yost GS. Calcium-dependent independent mechanisms of capsaicin receptor (TRPV1)-mediated cytokine production cell death in human bronchial epithelial cells. *J Biochem Mol Toxicol*. 2005; 19:266–275. [PubMed: 16173059]
21. Johansen ME, Reilly CA, Yost GS. TRPV1 antagonists elevate cell surface populations of receptor protein and exacerbate TRPV1-mediated toxicities in human lung epithelial cells. *Toxicol Sci*. 2006; 89:278–286. [PubMed: 16120755]
22. Reilly CA, Taylor JL, Lanza DL, Carr BA, Crouch DJ, Yost GS. Capsaicinoids cause inflammation and epithelial cell death through activation of vanilloid receptors. *Toxicol Sci*. 2003; 73:170–181. [PubMed: 12721390]
23. Chuang H, Lin S. Oxidative challenges sensitize the capsaicin receptor by covalent cysteine modification. *Proc Natl Acad Sci*. 2009; 106:20097–20102. [PubMed: 19897733]
24. Hinman A, Chuang H, Bautista DM, Julius D. TRP channel activation by reversible covalent modification. *Proc Natl Acad Sci*. 2006; 103:19564–19568. [PubMed: 17164327]
25. Fernandez-Ballester G, Ferrer-Montiel A. Molecular modeling of the full-length human TRPV1 channel in closed and desensitized states. *J Membrane Biol*. 2008; 223:161–172. [PubMed: 18791833]
26. Miyamoto T, Dubin A, Petrus M, Patapoutian A. TRPV1 and TRPA1 mediate peripheral nitric oxide-induced nociception in mice. *PloS ONE*. 2009; 4:e7596. [PubMed: 19893614]
27. Salazar H, Llorente I, Jara-Oseguera A, Garcia-Villegas R, Munari M, Gordon S, Islas L, Rosenbaum T. A single N-terminal cysteine in TRPV1 determines activation by pungent compounds from onion and garlic. *Nature Neurosci*. 2008; 11:255–261. [PubMed: 18297068]

28. Susankova K, Tousova K, Vyklicky L, Teisinger J, Vlachova V. Reducing and oxidizing agents sensitize heat-activated vanilloid receptor (TRPV1) current. *Mol Pharmacol*. 2006; 70:383–394. [PubMed: 16614139]
29. Grandl J, Hu H, Bandell M, Bursulaya B, Schmidt M, Petrus M, Patapoutian A. Pore region of TRPV3 ion channel is specifically required for heat activation. *Nature Neuroscience*. 2008; 11:1007–1013.
30. Aneiros E, Cao L, Papakosta M, Stevens E, Phillips S, Grimm C. The biophysical and molecular basis of TRPV1 proton gating. *EMBO J*. 2011; 30:994–1002. [PubMed: 21285946]
31. Oseguera A, Islas L, Garcia-Villegas R, Rosenbaum T. On the mechanism of TBA block of the TRPV1 channel. *Biophysical Journal*. 2007; 92:3901–3914. [PubMed: 17369424]
32. Friedman M. Chemistry, nutrition, and microbiology of D-amino acids. *J Agric Food Chem*. 1999; 47:3457–3479. [PubMed: 10552672]

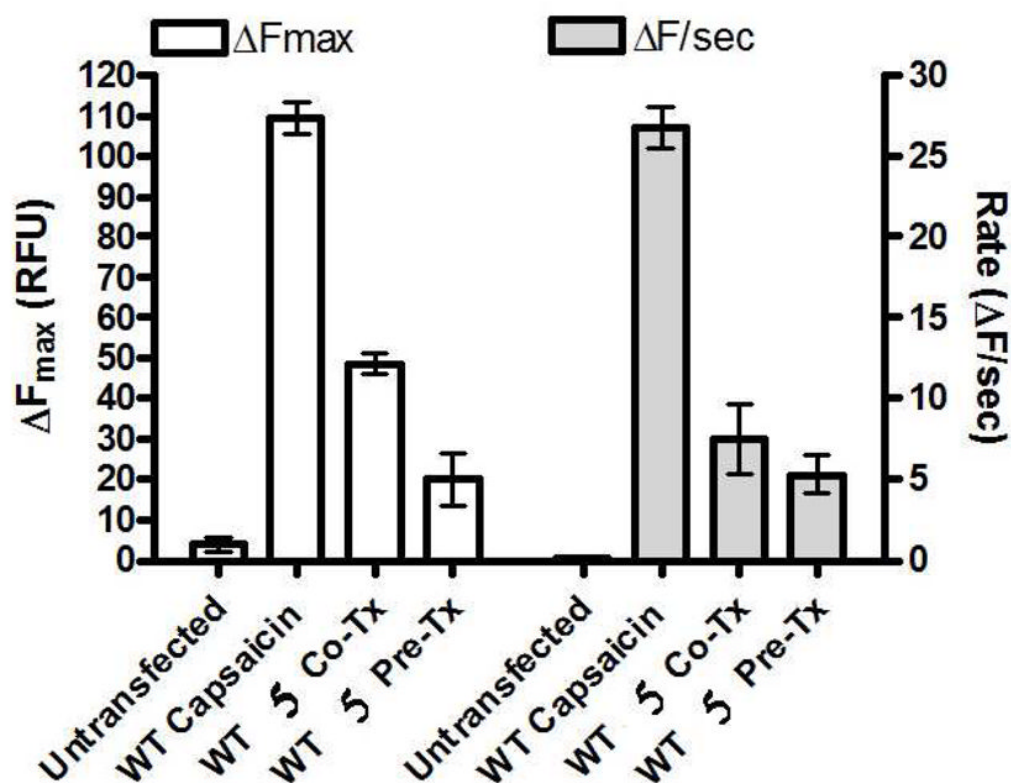


Figure 1.

Time-dependent inhibition of TRPV1 by **5**. HEK-293 cells were transfected with human wild type TRPV1 and pre-treated with compound **5** (375 μM), followed by application of capsaicin (25 μM). For comparison, cells were co-treated with both agents. The change in fluorescent response to Ca^{2+} (ΔF) was measured as a function of maximum fluorescence or of fluorescence rate ($n=3$).

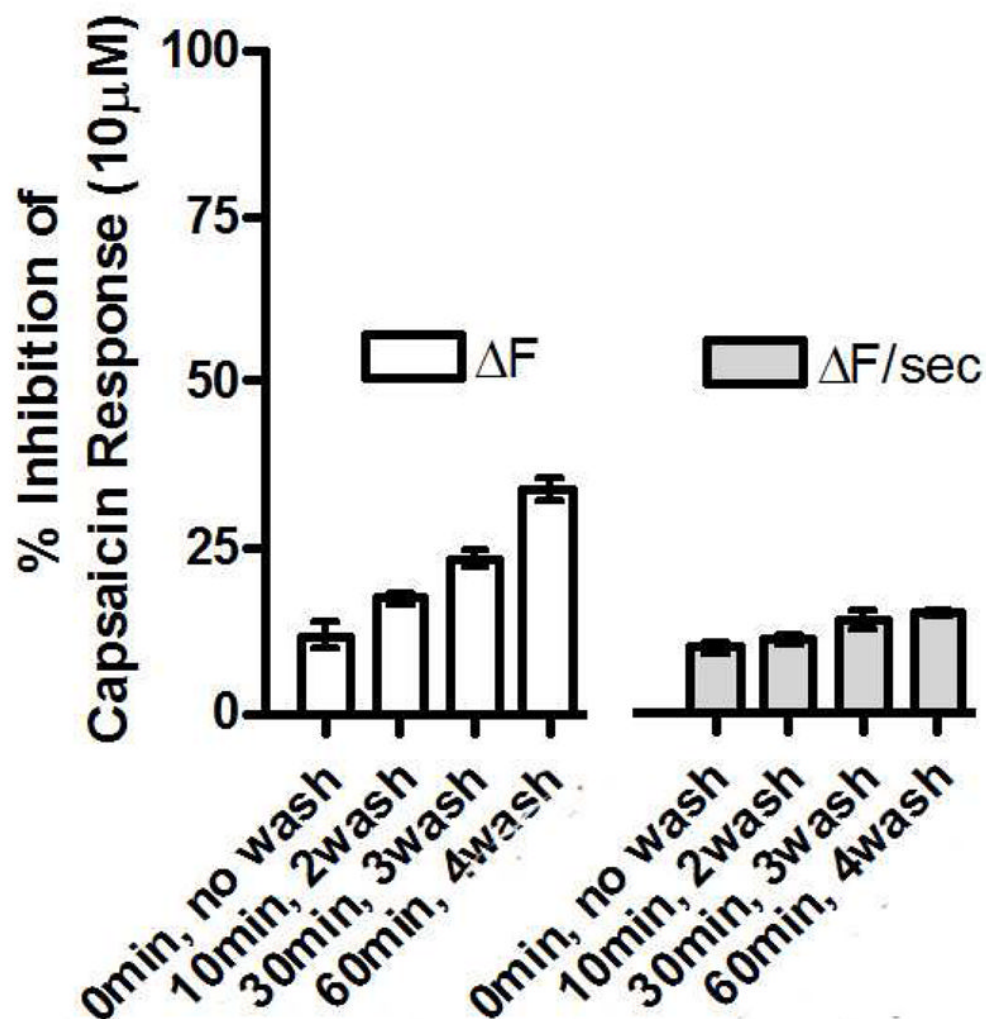


Figure 2. Stability of TRPV1 inhibition. Compound 2 ($375\mu\text{M}$) was incubated with HEK-293 cells transfected with wild-type human TRPV1. Response to capsaicin was measured over a 1 h timecourse with washes at various intervals (x-axis). The change in fluorescent response to Ca^{2+} (ΔF) was measured as a function of maximum fluorescence or of fluorescence rate.

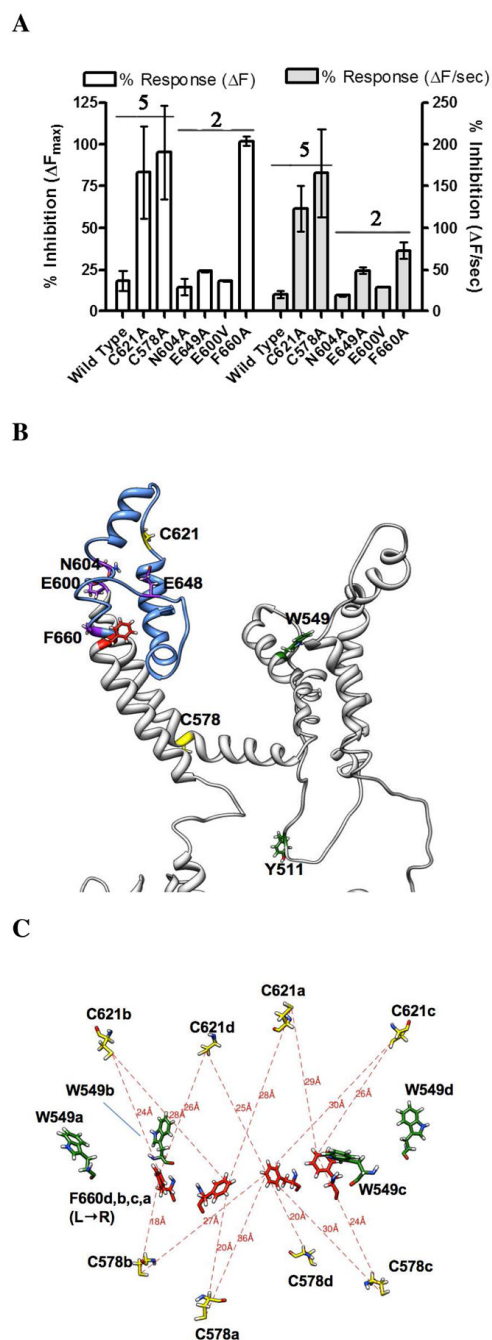


Figure 3.

Mutational analysis of human TRPV1 inhibition. **A.** Compounds **2** ($375\mu\text{M}$) and **5** ($375\mu\text{M}$) were pre-incubated with HEK-293 cells transfected with wild-type and mutant TRPV1 channels. Inhibition of the capsaicin response was compared. The change in fluorescent response to Ca^{2+} (ΔF) was measured as a function of maximum fluorescence or of fluorescence rate. **B.** Side view of a homology model of a single subunit of human TRPV1.²⁵ Highlighted residues involved in capsaicin binding (green) and nobilamide binding (yellow: Cys; red: Phe), as well as residues whose mutation does not affect nobilamide binding. **C.** Side view of a homology model of the TRPV1 tetramer pore loop region showing residues and intra-molecular distance between residues involved in

capsaicin or nobilamide binding (colors as in B). The ion pore runs through the middle of this diagram and is presumably blocked by nobilamide binding between F660 and/or C578 and C621, either within or between subunits of the functional tetramer.

Table 1

¹H (500 MHz) NMR Data for Nobilamides A-H (4-11) in DMSO-*d*₆

unit	No	4	5	6	7	8	9	10 ^a	11 ^a
		δ_H (J in Hz)	δ_H (J in Hz)	δ_H (J in Hz)	δ_H (J in Hz)	δ_H (J in Hz)	δ_H (J in Hz)	δ_H (J in Hz)	δ_H (J in Hz)
Z-Dhb	3	6.53 q (7.1)	6.58 q (7.0)	-	6.71 q (6.7)	6.69 q (7.2)	6.69 q (7.5)	6.89 δ (7.8)	6.89 δ (6.6)
	4	1.59 d (7.1)	1.64 d (7.0)	-	1.64 d (7.2)	1.63 d (7.2)	1.63 d (7.5)	1.73 d (7.8)	1.73 d (6.6)
NH		8.99 s	9.04 brs	-	8.29 s	8.28 s	8.33 m		
L-Ala	2	4.38 m	4.43 m	4.17 m	4.28 m	4.27 m	4.23 m	4.46 m	4.44 m
	3	1.25 d (7.1)	1.31 d (7.0)	1.25 d (7.3)	1.30 d (7.3)	1.31 m	1.34 d (7.0)	1.37 d (6.5)	1.42 d (6.9)
NH		8.14 d (7.0)	8.19 d (7.7)	7.97 d (7.7)	7.94 d (9.0)	8.02 m	8.33 m		
L-Val	2	4.25 dd (6.7, 8.2)	4.30 dd (6.5, 8.5)	4.25 dd (7.0, 8.7)	3.89 m	3.90 dd (7.0, 8.0)	3.96 dd (1.0, 9.7)	4.03 m	4.03 m
	3	1.98 m	2.03 m	1.97 m	1.94 m	1.93 m	2.01 m	2.04	2.12 m
	4/5	0.81 d (6.7); 0.84 d (6.7)	0.86 d (6.0); 0.88 d (6.0)	0.87 d (6.6); 0.83 d (6.6)	0.84 d (7.0); 0.75 d (7.0)	0.83 d (6.9); 0.76 d (6.9)	0.87 d (6.7); 0.83 d (6.7)	0.96 d (6.5); 0.95 d (6.5)	0.97 d (7.0); 0.95 d (7.0)
NH		7.70 d (8.6)	7.75 (8.5)	7.70 d (9.3)	7.51 d (9.3)	7.62 brs	8.10 d (10.0)		
D-a-Thr	2	4.30 dd (7.6, 7.6)	4.36 dd (7.0, 7.2)	4.31 dd (7.8)	4.15 m	4.03 d (5.6)	4.05 m	4.19 brs	4.22 brs
	3	3.78 m	3.83 m	3.78 m	4.72 q (6.6)	4.60 m	4.51 m	4.57 m	4.50 m
	4	1.01 d (6.3)	1.07 d (5.8)	1.01 d (6.1)	1.36 d (6.6)	1.30 m	1.30 d (6.3)	1.43 d (6.8)	1.38 d (7.0)
NH		8.09 d (8.7)	8.14 d (8.6)	8.10 d (8.5)	8.47 d (7.0)	8.32 m	8.33 m		
L-Phe (L-Tyr)	2	4.58 m	4.59 m	4.58 m	4.47 m	4.41 m	4.06 m	3.30 m	3.39 t (7.9)
	3	3.07 dd (3.5, 13.4); 2.70 dd (11.5, 13.4)	3.06 dd (2.0, 13.4); 2.71 m	3.06 dd (3.5, 13.4); 2.70 dd (11.5, 13.4)	3.05 dd (4.8, 13.3); 2.84 dd (10.0, 13.3)	2.94 m, 2.70 m	3.05 m	2.89 m	2.89 m
	ph	7.12~7.29 m	7.02~7.30 m	7.12~7.29 m	7.07~7.29 m	7.00 d (8.4); 6.62 d (8.0)	7.19~7.37 m	7.19~7.37 m	7.19~7.37 m
NH		8.26 d (8.6)	8.28 d (8.4)	8.26 d (9.4)	8.42 d (7.9)	8.30 m	8.81 d (7.0)		
D-Leu	2	4.18 m	4.20 m	4.16 m	-	4.20 m	-	Propanone	Propanone
	3	1.15 m	1.15 m	1.14 m	-	1.26 m	-	1 3.42 m	3.27 m
	4	1.16 m	1.16 m	1.15 m	-	1.27 m	-	3 2.14 s	2.09 s
	5/6	0.72 d (5.5); 0.69 d (5.5)	0.73 d (5.6); 0.70 d (5.6)	0.72 d (5.5); 0.69 d (5.5)	-	0.79 d (6.2); 0.75 m	-	4 1.17 d (7.0)	1.21 d (6.9)
NH		7.98 d (7.4)	7.92 d (8.0)	8.28 d (7.7)	-	7.99 m	-	-	-
D-Phe	2	4.47 m	4.48 m	4.47 m	4.48 m	4.52 m	-	-	-

unit	No	4	5	6	7	8	9	10 ^a	11 ^a
		δ_H (J in Hz)	δ_H (J in Hz)	δ_H (J in Hz)	δ_H (J in Hz)	δ_H (J in Hz)	δ_H (J in Hz)	δ_H (J in Hz)	δ_H (J in Hz)
	3	2.91 d (3.4, 13.9); 2.65 dd (10.3, 13.9)	2.93 dd (3.0, 13.7); 2.69 m	2.90 d (3.4, 13.9); 2.65 dd (10.3, 13.9)	2.74 dd (4.0, 13.4); 2.52 dd (10.2, 13.4)	2.97 m; 2.67 m	-	-	-
ph		7.12~7.29 m	7.0~7.3 m	7.12~7.29 m	7.07~7.29 m	7.14~7.26 m	-	-	-
NH		8.01 d (8.2)	7.91d (8.0)	8.02 d (8.5)	7.92 d (8.1)	7.88 brs	-	-	-
Fatty acid	2	1.70 s	1.98 m	1.71 s	1.70 s	1.78 s	-	-	-
	3	-	0.82 m	-	-	-	-	-	-

^a data were measured in CD₃OD-*d*₄

Table 2

¹³C (125 MHz) NMR Data for Nobilamides A-H (4–11) in DMSO-*d*₆

unit	No	4	5	6	7	8	9	10 ^a	11 ^a
		δ_C (mult.)	δ_C (mult.)	δ_C (mult.)	δ_C (mult.)	δ_C (mult.)	δ_C (mult.)	δ_C (mult.)	δ_C (mult.)
Z-Dhb	1	166.1 qC	166.0 qC	-	163.2 qC	163.5 qC	163.1 qC	165.3 qC	165.3 qC
	2	129.4 qC	128.5 qC	-	126.0 qC	126.3 qC	126.2 qC	128.0 qC	127.9 qC
	3	133.8 CH	132.6 CH	-	133.8 CH	134.2 CH	134.1 CH	138.9 CH	138.7 CH
	4	15.8 CH ₃	14.2 CH ₃	-	15.3 CH ₃	15.5 CH ₃	15.2 CH ₃	15.7 CH ₃	15.7 CH ₃
L-Ala	1	171.5 qC	171.4 qC	174.6 qC	170.1 qC	170.1 qC	168.7 qC	173.1 qC	173.2 qC
	2	50.0 CH	48.7 CH	52.1 CH	50.0 CH	50.2 CH	50.3 CH	51.8 CH	52.0 CH
	3	19.9 CH ₃	18.3 CH ₃	17.8 CH ₃	17.9 CH ₃	17.9 CH ₃	17.8 CH ₃	18.6 CH ₃	19.1 CH ₃
L-Val	1	171.2 qC	171.0 qC	171.8 qC	171.3 qC	171.3 qC	170.2 qC	174.8 qC	174.5 qC
	2	59.0 CH	57.7 CH	57.7 CH	61.4 CH	61.5 CH	61.8 CH	64.1 CH	64.4 CH
	3	32.6 CH	31.0 CH	31.5 CH	28.6 CH	29.2 CH	28.9 CH	31.3 CH	31.1 CH
	4/5	21.3/19.8 CH ₃	19.5/18.3 CH ₃	20.1/18.9 CH ₃	19.5/19.4 CH ₃	19.8/19.5 CH ₃	19.6/19.9 CH ₃	20.8/20.4 CH ₃	20.7/20.3 CH ₃
D- α -Thr	1	170.4 qC	170.2 qC	170.3 qC	168.1 qC	168.0 qC	167.4 qC	171.4 qC	171.3 qC
	2	60.2 CH	59.1 CH	59.1 CH	57.6 CH	58.3 CH	58.1 CH	59.0 CH	59.3 qC
	3	68.8 CH	67.7 CH	67.9 CH	73.9 CH	73.4 CH	73.9 CH	76.4 CH	76.3 CH
	4	21.8 CH ₃	20.4 CH ₃	20.7 CH ₃	17.9 CH ₃	17.8 CH ₃	17.5 CH ₃	17.7 CH ₃	19.2 CH ₃
L-Phe (L-Tyr)	1	171.8 qC	171.8 qC	171.3 qC	171.9 qC	172.2 qC	171.4 qC	177.1 qC	177.1 qC
	2	55.9 CH	54.0 CH	54.7 CH	55.0 CH	55.2 CH	54.0 CH	64.9 CH	64.4 CH
	3	39.5 CH ₂	38.2 CH ₂	38.5 CH ₂	38.2 CH ₂	37.0 CH ₂	37.3 CH ₂	42.0 CH ₂	41.8 CH ₂
	4	138.7 qC	138.6 qC	138.7 qC	137.7 qC	130.6 qC	135.1 qC	139.8 qC	139.4 qC
	5,9	128.7 CH	128.4 CH	128.7 CH	128.0 CH	127.9 CH	129.0 CH	130.4 CH	130.4 CH
	6,8	129.9 CH	129.7 CH	129.9 CH	129.1 CH	115.3 CH	129.8 CH	131.2 CH	131.2 CH
	7	126.8 CH	126.7 CH	126.8 CH	126.5 CH	156.5 qC	127.8 CH	128.8 CH	128.9 CH
D-Leu	1	172.4 qC	172.2 qC	172.4 qC	-	172.6 qC	-	Propanone	Propanone
	2	53.1 CH	51.9 CH	48.3 CH	-	52.1 CH	-	1 64.7 CH	64.6 CH
	3	42.7 CH ₂	41.3 CH ₂	41.8 CH ₂	-	41.5 CH ₂	-	2 215.3 qC	214.2 qC
	4	25.8 CH	26.3 CH	24.8 CH	-	24.2 CH	-	3 27.8 CH ₃	26.2 CH ₃

unit	No										11 ^a	
		4	5	6	7	8	9	10 ^a	11 ^a			
		δ_C (mult.)	δ_C (mult.)	δ_C (mult.)	δ_C (mult.)	δ_C (mult.)	δ_C (mult.)	δ_C (mult.)	δ_C (mult.)	δ_C (mult.)	δ_C (mult.)	δ_C (mult.)
	5/6	23.8/24.7 CH ₃	22.8/22.6 CH ₃	23.5/22.6 CH ₃	-	19.5/23.5 CH ₃	-	4 19.3 CH ₃	17.6 CH ₃			
D-Phe	1	172.0 qC	171.6 qC	172.2 qC	172.0 qC	171.6 qC	-	-	-	-	-	-
	2	55.5 CH	54.7 CH	54.5 CH	54.6 CH	54.1 CH	-	-	-	-	-	-
	3	39.0 CH ₂	37.7 CH ₂	38.1 CH ₂	37.6 CH ₂	37.6 CH ₂	-	-	-	-	-	-
	4	138.6 CH	138.5 qC	138.6 CH	137.4 qC	138.2 qC	-	-	-	-	-	-
	5,9	128.6 CH	128.0 CH	128.6 CH	128.0 CH	128.4 CH	-	-	-	-	-	-
Fatty acid	6,8	129.8 CH	129.0 CH	129.8 CH	129.0 CH	130.1 CH	-	-	-	-	-	-
	7	126.8 CH	126.7 CH	126.8 CH	126.2 CH	126.7 CH	-	-	-	-	-	-
	1	169.9 qC	173.4 qC	169.9 qC	169.9 qC	169.7 qC	-	-	-	-	-	-
	2	24.3 CH ₃	28.6 CH ₃	23.3 CH ₃	22.9 CH ₃	23.2 CH ₃	-	-	-	-	-	-
	3	-	10.3 CH ₃	-	-	-	-	-	-	-	-	-

^a data were measured in CD₃OD-*d*₄